

## ORIGINAL PAPER

# Synthesis by UV-curing and characterisation of polyurethane acrylate-lithium salts-based polymer electrolytes in lithium batteries

Mustafa Hulusi Ugur, Hasan Kılıç, Mustafa Lütfü Berkem, Atilla Güngör\*

*Department of Chemistry, Marmara University, Fen Edebiyat Fakültesi Göztepe Kampüsü, 34722, Kadıköy – İstanbul, Turkey*

Received 27 November 2013; Revised 23 April 2014; Accepted 24 April 2014

UV-cured caprolactone-based polyurethane acrylate (PUA) polymer blend electrolytes were prepared and characterised. To develop polymer electrolytes suited to ambient temperature, an ionically-conductive and reliable polymer electrolyte based on urethane acrylate resins synthesised from a fluorine-containing di-functional oligomer 6F ethoxylated diacrylate, a di-functional reactive diluent 1,6-hexanediol diacrylate for adjusting the viscosity, and a radical photo-initiator doped with a mixture of lithium salts were used. Free-standing flexible electrolyte films were prepared by UV-curing via free-radical photopolymerisation. The performance of the lithium polymer cell system (Li/PE(F4)/LiCoO<sub>2</sub>) was determined by electrochemical impedance spectroscopy, cyclic voltammetry, a galvanostatic recurrent differential pulse, chronocoulometry and chronoamperometry. The electrolyte with optimal amounts of fluorine-containing oligomer and optimal salt mixture content exhibited enhanced conductivity, showing a conductivity of  $1.00 \times 10^{-4} \text{ S cm}^{-1}$  at ambient temperature. The specific capacity, specific energy and specific power of a Li/PE(F4)/LiCoO<sub>2</sub> cell were also determined.

© 2014 Institute of Chemistry, Slovak Academy of Sciences

**Keywords:** polymer blends, conducting polymers, membranes, polyurethanes

## Introduction

Today's environmentally aware consumers require reliable and non-toxic rechargeable battery products. Rechargeable batteries are key components in mobile technologies such as portable consumer electronics and electric vehicles. The energy characteristics of lithium secondary batteries render them attractive for use in electric vehicles in terms of reducing environmental pollution (Scrosati, 1993; Besenhard & Winter, 2002; Yang et al., 2011; Jia et al., 2012). Li<sup>+</sup> ions, which are an excellent choice for electrochemical power sources, are characterised by high energy and/or power densities, good cyclability, reliability and safety (Scrosati, 1995; Gerbaldi et al., 2009). In recent years, several cross-linked polymer electrolytes based on acrylates have been prepared using UV-based photopolymerisation (Oh et al., 2002; Gerbaldi et al., 2010; Kil et al., 2013). UV-curing, which is recognised as being easily performed, inex-

pensive, fast and reliable, was adopted for preparing the solid polymer electrolyte (Yildiz et al., 1995; Garino et al., 2013). UV-cured films need to be environmentally compliant. They must be non-toxic, non-polluting and safe when applied to lithium-based battery solutions.

In recent years, attention has focused on polymer/salt mixtures due to growing interest in these systems as rapid ion-conducting systems. Several types of lithium ion-conducting polymer electrolytes have been prepared as perfect homogenous mixtures of the components, namely polyethylene oxide (PEO), polyurethane acrylate (PUA) or polyimide (PI), as the polymer matrix capable of dissolving different alkali metal salts and lithium trifluoromethanesulphonate (LiCF<sub>3</sub>SO<sub>3</sub>), lithium tetrafluoroborate (LiBF<sub>4</sub>) and lithium perchlorate (LiClO<sub>4</sub>) as a lithium salt (Papke et al., 1982; de Zea Bermudez et al., 1999; Silva et al., 2002; Johnson et al., 2013; Uğur et al., 2014).

In this study, four membranes with different con-

\*Corresponding author, e-mail: atillag@marmara.edu.tr

centrations of ethoxylated-6F diacrylate, oligomers and lithium salt mixtures were prepared. Their ionic conductivities and electrochemical properties were characterised by electrochemical techniques. In addition, several experimental techniques, including thermogravimetric analysis (TGA), electrochemical impedance spectroscopy (EIS) and cyclic voltammetry (CV) were employed to determine the basic properties of the polymer membranes.

### Experimental

Caprolactone diol (CL diol,  $M_W = 2000 \text{ g mol}^{-1}$ ), 2-hydroxyethyl methacrylate (2-HEMA) and 1-methyl-2-pyrrolidone (NMP) and battery-grade ethylene carbonate (EC), dimethyl carbonate (DMC), propylene carbonate (PC) and lithium triflate ( $\text{LiCF}_3\text{SO}_3$ ) were purchased from Sigma–Aldrich (Germany). Hexafluorinated (6F) bisphenol A was purchased from Dow Chemical (USA). 2,4- and 2,6-Toluene diisocyanate (TDI), dibutyltin dilaurate (DBTDL), lithium tetrafluoroborate ( $\text{LiBF}_4$ ) were purchased from Merck (Germany). 1,6-hexanediol diacrylate (HDDA) was purchased from DSM-AGI (Taiwan) and used as received. Polyvinylidene fluoride-*co*-hexafluoropropylene (PVdF–HFP,  $M_n = 130000 \text{ g mol}^{-1}$ ) was used after purification. Acetylene black was purchased from Alfa Aesar (Germany) and used after purification. The photo-initiator (1-hydroxycyclohexyl phenyl ketone-Irgacure 184) was purchased from Ciba Specialty Chemicals (Switzerland). TDI and 2-HEMA were distilled under vacuum. Prior to use, all chemicals were retained over molecular sieves in the inert atmosphere of an Ar-filled home-designed glove box (Ercom Kompresör, Istanbul, Turkey) for two days to remove traces of water from the oligomers. This was performed to

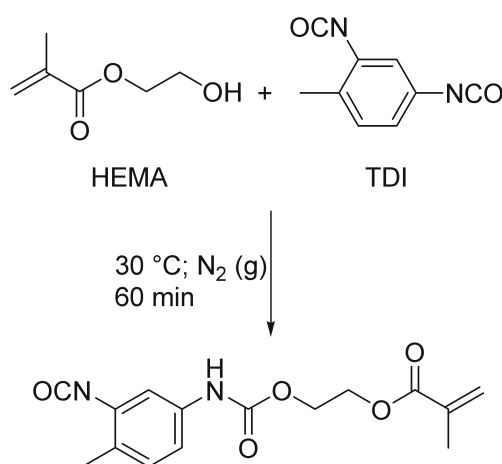


Fig. 1. Reaction scheme of HEMA-TDI product.

avoid problems when assessing the long-term properties of these membranes for application as electrolytes in rechargeable lithium batteries.

### Synthesis of polyurethane resin

There have been many reports on the synthesis of acrylated polyurethane resins (Lin et al., 1984; Yildiz et al., 1995). CL diol, 2-HEMA and a mixture of 2,4- and 2,6-TDI were used to synthesise the acrylated urethane oligomer. TDI and 2-HEMA were distilled under vacuum and THF was distilled prior to use. This reaction was performed in two steps under a nitrogen atmosphere. The reaction schemes are given in Figs. 1 and 2.

Step one: Anhydrous THF, TDI (5.22 g, 0.030 mole) and a catalyst (DBTDL, one drop) were poured

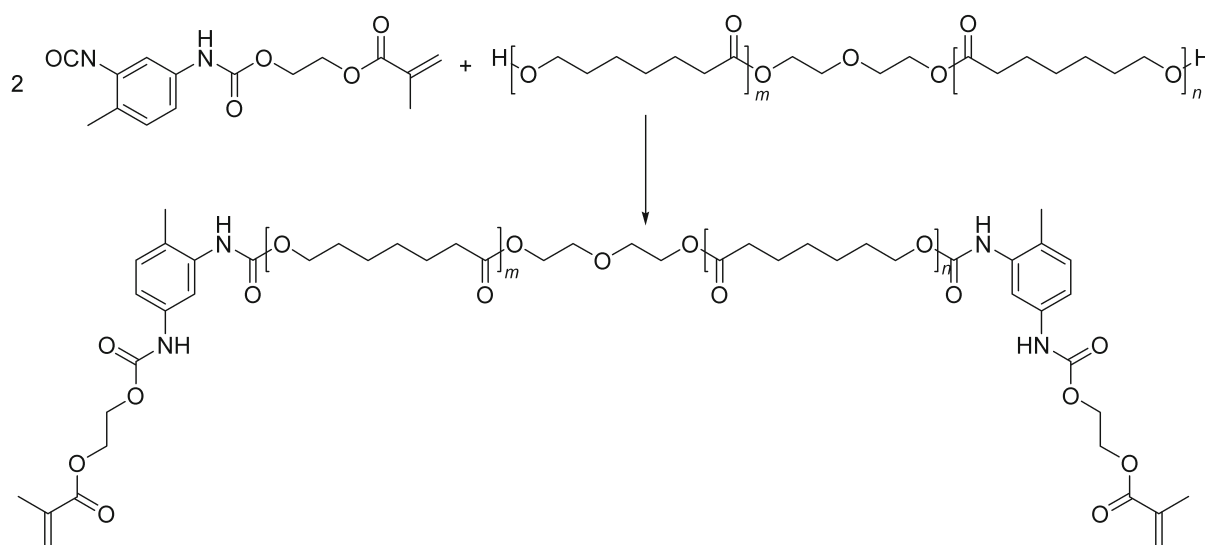


Fig. 2. Reaction scheme of urethaneacrylate oligomer synthesis.

into a 250-mL thoroughly flame-dried three-necked reaction vessel equipped with a magnetic stirrer, thermometer, dropping funnel and gas inlet for dry nitrogen. The reaction vessel was then placed in a water bath for temperature control. During this step, the reaction temperature was set at 30 °C. Next, 2-HEMA (3.9 g, 0.030 mole) was gradually added to the reaction vessel through the dropping funnel. The reaction continued until complete elimination of the —OH absorption peak of 2-HEMA and formation of the —NH— absorption peak in the IR spectrum. The reaction time for this step was 60 min.

Step two: CL diol (30 g, 0.015 mole) was slowly added through the dropping funnel to the reaction vessel containing the product from the first step. The reaction temperature was 50 °C and the reaction proceeded until the complete disappearance of the —NCO absorption peak while the absorption peak of —NH— in the FTIR spectrum steadily increased (Fig. 6b). The reaction time for this step was 150 min. At the end of the reaction, THF was removed by vacuum distillation. A viscous liquid was obtained.

#### Synthesis of ethoxylated-6F and 6F diacrylate

Ethoxylated-6F was synthesised by the bulk reaction of 6F bisphenol A (15 g, 0.0445 mole) with EC (9.45 g, 0.0979 mole) in the presence of 0.69 g (0.0022 mole) tetraethylammonium iodide ( $\text{N}(\text{C}_2\text{H}_5)_4^+ \text{I}^-$ ) in a molar ratio of 1 : 2.2 : 0.05, respectively (Fig. 3). The reaction was completed within approximately 4 h. Thin-layer chromatography (TLC) and FTIR (Fig. 6a) were used to confirm completion of the reaction. Following the purification of ethoxylated-6F, the product was kept overnight in a vacuum oven at 80 °C (Gunduz, 1998; Kayaman-Apohan et al., 2005).

The ethoxylated-6F diacrylate was synthesised by the esterification reaction of ethoxylated-6F (14 g, 0.033 mole) with acryloyl chloride (5.6 mL, 0.069 mole) in the presence of 7.35 g (0.0726 mole) of triethylamine (TEA) as acid scavenger and 4-dimethyl-

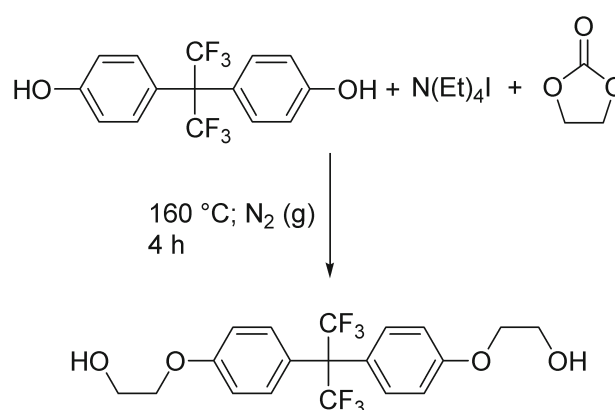


Fig. 3. Reaction scheme for synthesis of ethoxylated 6F.

aminopyridine (0.21 g, 0.00165 mole) as catalyst in a molar ratio of 1 : 2.1 : 2.2 : 0.05, respectively, as in the procedure previously reported (Fig. 4) (Gunduz, 1998).

#### Preparation of free-film formulations and casting free-films

Typically, plasticisers behave act as solvents when mixed with a polymer. This results in a reduction in the  $T_g$  value. This effect is related to a weakening of the dipole – dipole interactions between the polymer chains, thereby helping to soften the polymer backbone and increase its segmental motion. In addition,  $\text{LiBF}_4$  exhibits high ionic conductivity but this decreases at low temperatures (Zhang et al., 2002).  $\text{LiCF}_3\text{SO}_3$  exhibits low ionic conductivity but very stable temperature dependence. Hence, in this case a mixture of  $\text{LiBF}_4$ – $\text{LiCF}_3\text{SO}_3$ , which demonstrated good properties, was used. The non-aqueous electrolytic solution was prepared by dissolving 1 M of  $\text{LiBF}_4$ – $\text{LiCF}_3\text{SO}_3$  in a molar ratio of 3 : 1 in 100 mL of an organic solvent mixture of EC, DMC and PC in a volume ratio of 50 : 25 : 25. The electrolyte solution

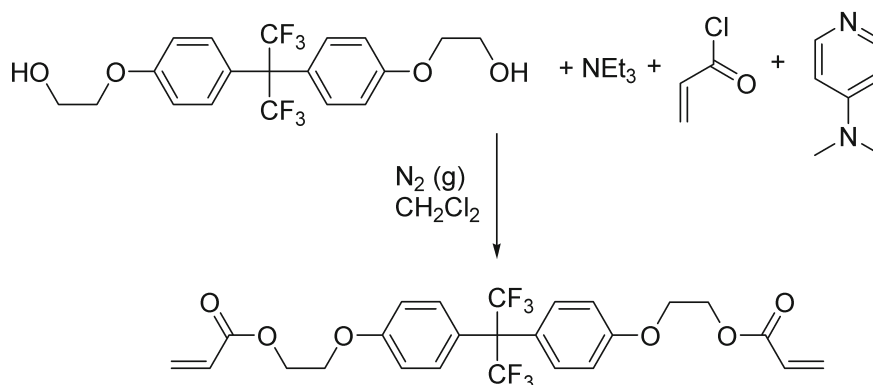


Fig. 4. Reaction scheme for acrylation of ethoxylated 6F.

**Table 1.** Formulation of UV-curable polymer resin

No.	Ingredient	Mass/%	Function
1	PUA	77	Oligomer
2	HDDA	20	Reactive diluent as cross-linking monomer
3	IRG.184	3	Photo-initiator
4	BYK088	One drop	Anti-foaming agent

PUA = polyurethane acrylate; HDDA = 1,6-hexanediol diacrylate; Irg.184 = Irgacure 184 (1-hydroxycyclohexyl phenyl ketone).

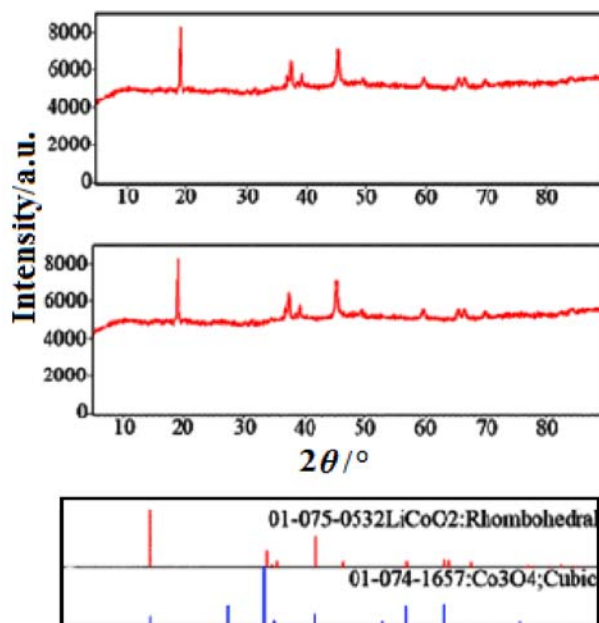
preparation and remaining processes were performed in a home-designed glove box. EC–DMC–PC solutions were used as plasticisers and Irgacure 184 was used as the free-radical photo-initiator.

A mixture of CL diol-based urethane acrylate oligomer, HDDA and Irgacure 184 was prepared. Table 1 shows the composition of the UV curable polymer resin. One gram of the solution thus obtained was added to 1 g of the liquid electrolyte solution. The resulting mixture was mixed for a minimum of 3 h for it to become sufficiently homogenous. The mixture was then cast onto a Mylar film at a thickness of approximately 150  $\mu\text{m}$  using a doctor-blade method. UV rays were directed onto the film with a 300 W UV lamp (OSRAM,  $\lambda_{\text{max}} = 365 \text{ nm}$ ) for approximately 5 min to induce polymerisation of the oligomer. This was performed in order to obtain a uniform UV-cured multi-component polymer blend electrolyte. The UV-cured films were transparent and yellow. The membranes were removed from the mould and used for further studies. To exclude the effects of moisture and oxygen, all the above processes were performed at humidity levels below 10–100 ppm (10–100  $\mu\text{L L}^{-1}$ ) at ambient temperature inside a home-designed glove box.

#### Preparation of cathode-active material and composite cathode material

PVdF–HFP was used after purification and dried in a vacuum oven at 80  $^{\circ}\text{C}$  for 24 h. Acetylene black was used after purification following a method previously reported (Armarego & Perin, 2002). Acetylene black was then leached for 24 h with concentrated HCl (1 g of acetylene black and 1 mL of conc. HCl) to remove oil contamination and washed repeatedly with distilled water. The acetylene black was dried in air and eluded for one day with benzene and one day with acetone. It was again dried in air at ambient temperature and heated in a vacuum oven at 600  $^{\circ}\text{C}$  for 24 h to remove the absorbed gases.

Lithium cobalt oxide ( $\text{LiCoO}_2$ ) is commonly used in rechargeable lithium batteries as a cathode-active material synthesised by a sol–gel method.  $\text{LiCoO}_2$  was prepared using stoichiometric amounts of reactants, e.g.  $\text{LiNO}_3$  and  $\text{Co}(\text{NO}_3)_2 \cdot 6\text{H}_2\text{O}$ . First, the reactants were dissolved in distilled water, thereby affording a nitrate metal solution. Next, poly(vinyl alcohol) was added as the gel agent. Finally, nitric acid was added

**Fig. 5.** XRD  $\theta/2\theta$  spectra of  $\text{LiCoO}_2$ .

to the solution to adjust the pH. This solution was continuously drained without any previous thermal dehydration at 100–150  $^{\circ}\text{C}$  in a drying oven prior to calcination, affording a viscous gel. This product was heated at 650  $^{\circ}\text{C}$  for 12 h. In the experiment for the initial mixtures of  $\text{LiNO}_3$  and  $\text{Co}(\text{NO}_3)_2 \cdot 6\text{H}_2\text{O}$ , in the binary phase, the compounds  $\text{LiCoO}_2$  and  $\text{Co}_3\text{O}_4$  were characterised by XRD analysis of the experimental products. The XRD analysis is shown in Fig. 5.

A mixture of 86.2 mass % of cathode-active material ( $\text{LiCoO}_2$ ), 8.6 mass % of PVdF–HFP as a binder and 5.2 mass % of acetylene black was prepared. The addition of the acetylene black conductor facilitates the migration of electrons. Then, a 100 mL of a mixture of NMP was transferred into a 250 mL plastic bottle and stirred for 24 h. The resulting mixture was cast onto a 40- $\mu\text{m}$ -thick aluminium and soft stainless steel foils rolled by a 150- $\mu\text{m}$ -spaced doctor-blade. The cast was dried in an oven at approximately 110  $^{\circ}\text{C}$  for approximately 12 h to completely evaporate the NMP. It was then pressed and cut to a predetermined size to form a cathode plate with a thickness of approximately 150  $\mu\text{m}$ .

The FTIR spectrum was recorded on a Perkin–

Elmer Spectrum 100 ATR-FTIR spectrophotometer (USA).

The structure of the LiCoO<sub>2</sub> powder was determined using a Bruker 8D Advance X-ray diffractometer with CuK<sub>α</sub> radiation. The data were collected in the 2θ range of 10–90 °C at a scan rate of 2° min<sup>-1</sup>.

The thermal stability of the samples was tested in the temperature range of 30–750 °C by thermogravimetric analysis (TGA) using a Perkin–Elmer STA 6000 instrument (Perkin–Elmer, USA) under N<sub>2</sub> flux at a heating rate of 10 °C min<sup>-1</sup>. Differential scanning calorimetry (DSC) measurements were carried out with a Perkin–Elmer Pyris Diamond (Perkin–Elmer, USA). The samples were analysed under a nitrogen atmosphere in the temperature range of –100–200 °C at a heating rate of 10 °C min<sup>-1</sup> and a cooling rate of 100 °C min<sup>-1</sup>.

Standard tensile stress-strain experiments were performed at ambient temperature on a Materials Testing Machine Z010/TN2S (Zwick, Germany) using a crosshead speed of 5 mm min<sup>-1</sup>. The mechanical properties of the polymer electrolytes were determined by standard tensile stress-strain tests in order to measure tensile strength and elongation at break. The specimen dimensions were 60.00 mm in length and 8.00 mm in width. Four parallel measurements were carried out for each sample. The gel content of the UV-cured films was determined by Soxhlet extraction with acetone for 6 h. Insoluble gel fractions were dried in an oven under vacuum at 50 °C until they were of a constant mass. In order to study the water absorption, all of the membranes were first soaked in distilled water at ambient temperature for 24 hours. The swollen membranes were removed from the distilled water, wiped gently with filter paper to remove any surface water and weighed (*W<sub>S</sub>*). All of the swollen membranes were kept at 70 °C overnight after which the dried membranes were weighed (*W<sub>D</sub>*). Finally, the water absorption in percent was calculated using the equation:

$$\text{Water absorption} = 100(W_S - W_D)/W_D \quad (1)$$

### EIS measurements

The conductivity of the UV-cured polymer electrolytes (PEs) was measured using electrochemical impedance spectroscopy (EIS). The PEs were placed between two Li electrodes in a Swagelok cell. The thickness of the electrolyte was measured before and after the EIS measurement to ensure a constant thickness. Ionic conductivity was measured under an argon atmosphere using a potentiostat/galvanostat and a home-made glove box with conductivity cell.

The *Z'* intercept of the semi-circle at higher frequency is related to the bulk resistance (*R<sub>b</sub>*) of the polymer membrane saturated with electrolyte. The diameter of the semi-circle at high frequency and

medium frequency is related to the interfacial resistance (*R<sub>i</sub>*) between the electrode and the polymer membrane saturated with the electrolyte (Morales & Acosta, 1999; Xu et al., 2001). The conductivity values of the polymer electrolyte systems are calculated from the intercept of the real part of the complex impedance plot, which is the resistance of the film and known area using the equation (Imperiya et al., 2013):

$$\sigma = L/RA \quad (2)$$

where *L/A* is the geometrical factor, *L* is the thickness of the UV-curable electrolyte film; *R* is the resistance of the UV-curable electrolyte film; and *A* is the area of the film.

### Electrochemical window stability – cyclic voltammetry (CV)

The stability window of the polymer electrolyte was evaluated by cyclic voltammetry using a three-electrode cell with a stainless steel foil (SS-Type 304) as the working electrode, a lithium foil as the reference and counter electrode and the given membrane as the electrolyte, respectively. A VoltaLab 80 PGZ-402 potentiostat/galvanostat (Gamry, USA) was used for the voltammetric measurements at a scan rate of 10 mV s<sup>-1</sup>.

### Electrochemical analysis

LiCoO<sub>2</sub> was chosen for the positive (cathode) electrode and lithium metal for the negative (anode) electrode. The cell was assembled in a casing, with the electrolyte sandwiched between the anode and cathode materials under an argon atmosphere in a glove box. The performance of the lithium polymer cell system (Li/PE(F4)/LiCoO<sub>2</sub>) was determined by a galvanostatic recurrent differential pulse, chronocoulometry and chronoamperometry with a Autolab potentiostat/galvanostat.

## Results and discussion

### FTIR analysis

Fig. 6 shows the FTIR spectrum of the urethane acrylate oligomer (a) and the HEMA-TDI product (b). The prominent peak observed at 2258 cm<sup>-1</sup> is characteristic of the isocyanate group (first-step intermediate in Fig. 6b). From the FTIR spectra, the disappearance of the characteristic absorption band at 2258 cm<sup>-1</sup> related to isocyanate (–NCO) indicates the completion of the reaction (a). As shown in Fig. 6a, the appearance of the strong characteristic peaks, such as the stretching vibrations of –NH at 3467 cm<sup>-1</sup>, the stretching vibrations of C=O at 1727 cm<sup>-1</sup>, the peak of C=C at 1669 cm<sup>-1</sup>, the deformation vibrations of

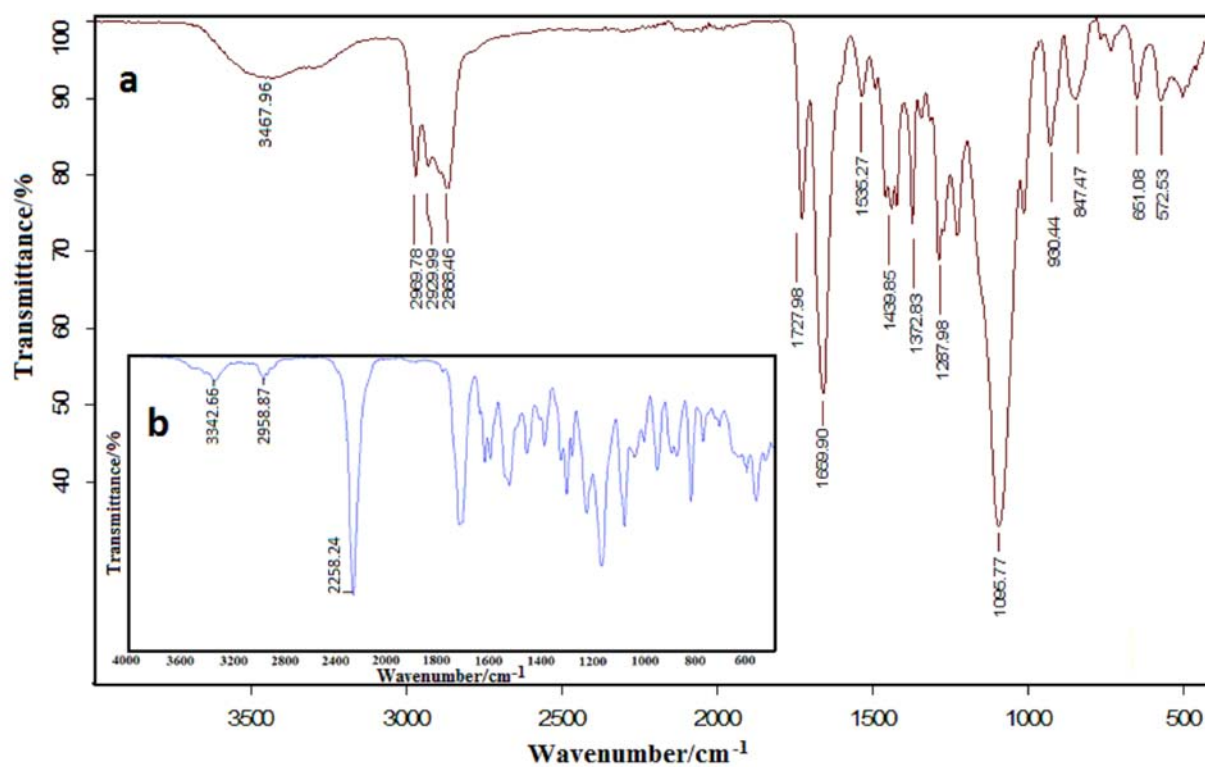


Fig. 6. FTIR spectra of urethane acrylate oligomer (a) and HEMA-TDI product (b).

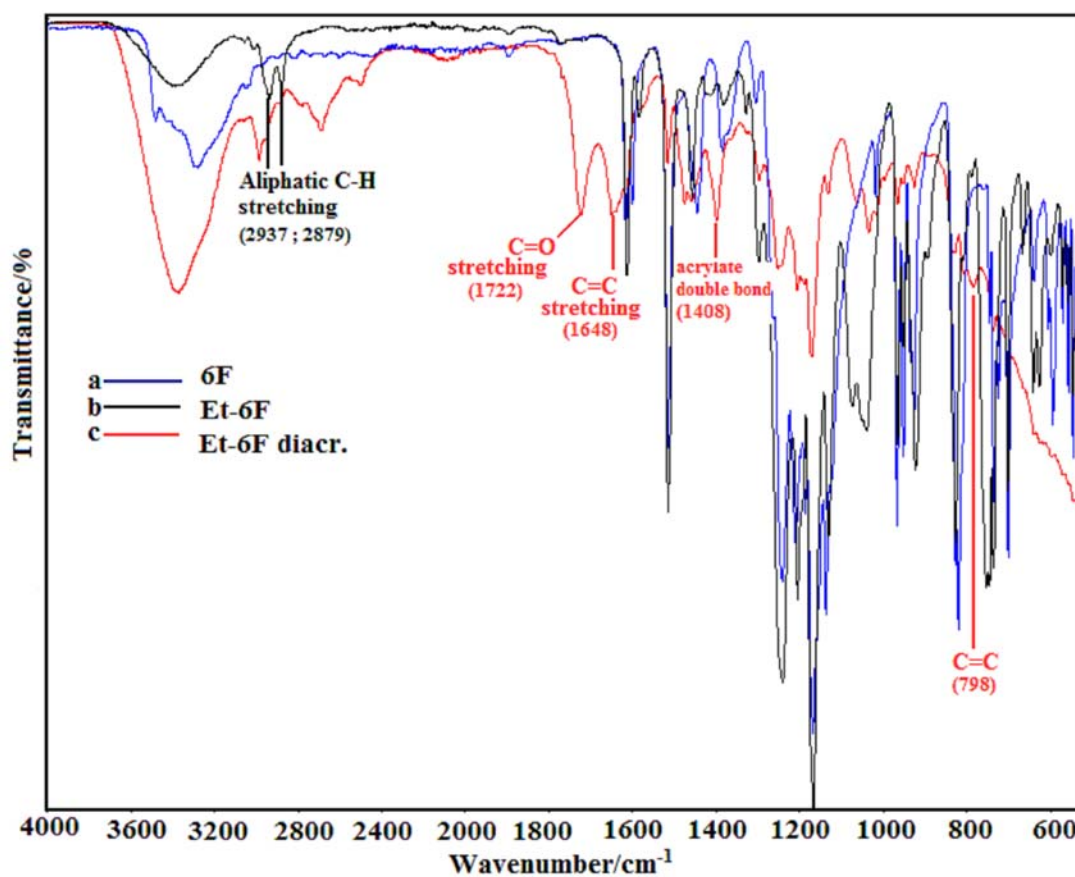


Fig. 7. FTIR spectra of 6F (a), ethoxylated 6F (b) and ethoxylated 6F diacrylate (c).

—NH at  $1535\text{ cm}^{-1}$ , the symmetric stretching for the C—O—C of the ester at  $1096\text{ cm}^{-1}$ , the C=C twisting of the acrylate at  $847\text{ cm}^{-1}$  and the stretching for the C—N at  $1287\text{ cm}^{-1}$  confirms the formation of PUA (Sultan et al., 2012; Panchal & Patel, 2013; Tabasum et al., 2013).

Fig. 7 shows the FTIR spectra of 6F (a), ethoxylated 6F (b) and ethoxylated 6F diacrylate (c). In all of these, the completion of the reaction is confirmed by the appearance of new peaks or changes in the intensities or shapes of the existing peaks in the FTIR spectra. Fig. 7b shows the aliphatic  $\text{CH}_2$  groups observed at  $2937\text{ cm}^{-1}$  and  $2879\text{ cm}^{-1}$  after the ethoxylation of 6F. A typical FTIR spectrum for ethoxylated BisA diacrylate is shown in Fig. 7c. The attachment of the polymerisable acrylate functional group by way of the process was indicated by the formation of the new carbonyl and acrylate peaks at around  $1722\text{ cm}^{-1}$  (carbonyl stretching),  $1648\text{ cm}^{-1}$ ,  $1408\text{ cm}^{-1}$  and  $798\text{ cm}^{-1}$ , respectively (Kang et al., 2003).

The disappearance of the reactive double bond upon UV radiation can be observed in the FTIR spectrum. It is known that, prior to UV irradiation, the FTIR spectrum of the acrylated polymer membranes exhibits unsaturated double bonds at  $1600\text{--}1650\text{ cm}^{-1}$ . Fig. 8 shows that, upon UV irradiation, the infrared absorption C=C stretching at around  $1650\text{--}1600\text{ cm}^{-1}$  disappears for the F4 membrane. Also, very tiny double bond absorptions can be seen at around  $1400\text{ cm}^{-1}$  due to some residual acrylic bonds in the 3D polymer matrix formed which are unable to react (Ali et al., 2001; Flåtten et al., 2005).

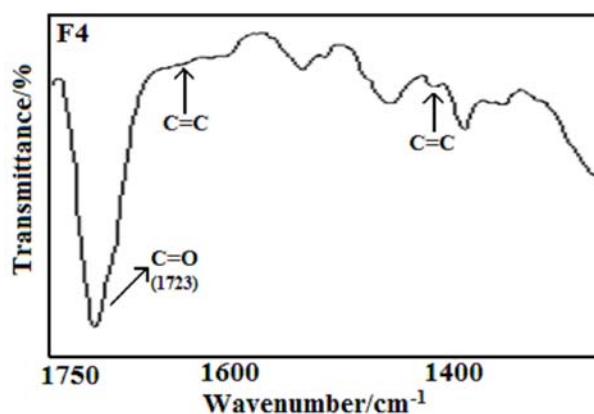


Fig. 8. FTIR spectra of UV-cured F4 membrane composed of PUA, ethoxylated 6F diacrylate and Li-salt solution. Curing time: 5 min.

### X-ray analysis

The predicted  $\text{LiCoO}_2$  powder diffraction positions are shown at the bottom. The spectrum reveals a polycrystalline structure of the  $\text{LiCoO}_2$  target. The  $\text{LiCoO}_2$  (003) peak at  $2\theta = 18.80^\circ$  is the strongest peak in Fig. 5. In addition, it is possible to make out the  $\text{LiCoO}_2$  (006) and (009) peaks, respectively at  $37.68^\circ$  and  $46.17^\circ$ , despite their being very weak.

### Thermal analysis

High ionic conductivity is a desirable property in battery applications; accordingly, membrane F4 was selected as the most promising membrane and further

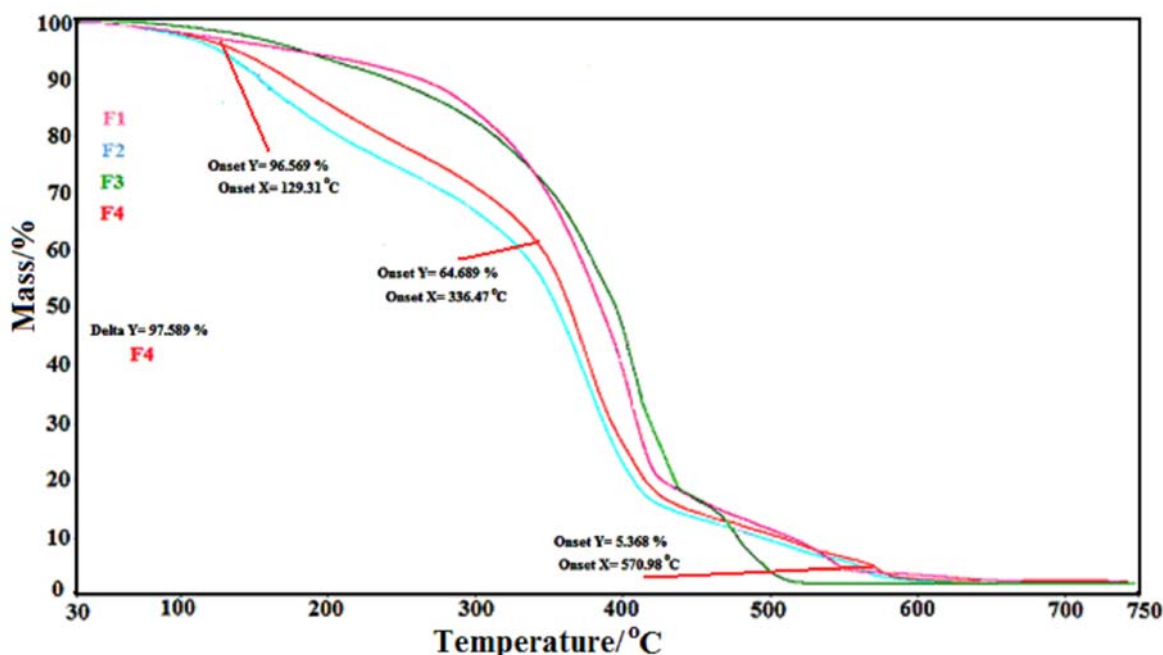


Fig. 9. TGA spectra of polymer electrolytes (F1–F4).

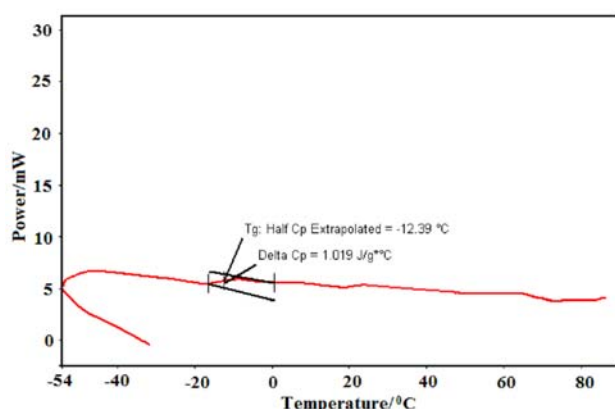


Fig. 10. DSC spectra of F4 membrane.

Table 2. Mechanical properties of UV-cured polymer electrolytes

Formulation	Tensile strength/MPa	Elongation at break/%
F1	0.7	10
F2	1.2	11
F3	1.5	9
F4	0.9	17

characterisation was focused on this membrane. Fig. 9 shows the TGA spectra of membranes F1–F4. In the derivative of all the TGA curves, four characteristic mass-loss peaks were observed. Fig. 9 also shows the TGA trace of membrane F4. It can be seen that a mass loss began at 130 °C for the F4 membrane, due to the partial removal of the alkyl carbonate solution and some solvent remaining. Generally, the first decomposition stage of PUA results from the degradation of urethane segments and the subsequent stage is due to the degradation of soft segments from the polyether or polyester (Gite et al., 2010; Seo et al., 2010). Hence, it is assumed that the second mass-loss peak corresponds to the urethane bond breakage, which occurs at between 250 °C and 360 °C in this UV-cured polymer electrolyte blend. (Şabani et al., 2012). The third is due to the decomposition of the ethoxylated 6F diacrylate-based aromatic structure at between 360 °C and 440 °C. Finally, the fourth mass-loss peak observed above 440 °C indicates the complete de-cross-linking and thermal degradation of the polymer (Athawale & Raut, 2002).

Fig. 10 shows the DSC spectra of membrane F4. The UV-cured membrane F4 was found to have a glass transition temperature value ( $T_g$ ) of  $-12.39$  °C.

### Mechanical properties of membranes

The properties of the UV-cured films were measured and the results are given in Table 2. UV-cured

films were found to have elongation at break values between 9 % and 17 %. In general, the polymer with a high degree of cross-linking density has a high mechanical strength but low extendability. It can be seen that the mechanical properties are closely dependent on the composition. On the other hand, the elongation at break of the UV-cured films increased on increasing the content of liquid electrolyte due to the plasticising effect on the polymer chain. The value of the elongation at break of F4 used in this study was found to be 17 %. This value is higher than the value found for other membranes; it can be attributed to the total Li-salt solution mass % in the formulation.

The UV-cured films were found to have tensile strength values between 0.7 and 1.5 MPa. It is known that the mechanical properties of the cross-linked polymers are highly dependent on the degree of cross-linking density. For the cross-linked polymer, the degree of cross-linking density strongly affected the mechanical properties such as tensile strength and maximum elongation (Kang et al., 2003; Santhosh et al., 2006). The tensile strength increased with the increasing content (mass %) of the ethoxylated sixF diacrylate in the polymer electrolytes.

The aromatic ring, the acrylate group and the optimal amount of Li-salt solution that are introduced to the cross-linker enhance the mechanical strength while sustaining high ion conductivity.

The hydrophilic character results in a relatively high water uptake, which is detrimental to the mechanical properties of the polymer electrolytes. Absorbed water molecules can act as a plasticiser to reduce the mechanical properties. In addition, polymeric systems containing aromatic structures with fluorine groups always exhibit excellent hydrophobicity. As previously reported, it was observed that dimethacrylates and/or diacrylates containing  $(CH_2)_n$  groups in the backbone generally yielded more desirable physical properties than those containing EO  $(CH_2CH_2O)_n$  groups (Kawaguchi et al., 1983; Gunduz, 1998). The degree of the cross-linking and hydrophobic character drastically affects the gel content and water absorption properties of UV-cured films. As shown in Table 3, the gel content (mass %) and water absorption values of UV-cured films were found to be 70–87 % and 2.4–8.5 %, indicating the formation of a three dimensional network structure. As the 6F diacrylate content (mass %) in the total formulation increases, the water absorption values decrease. This can be attributed to the decreasing percentage ratio of fluorine-containing electrolyte in the total structure.

### EIS measurements

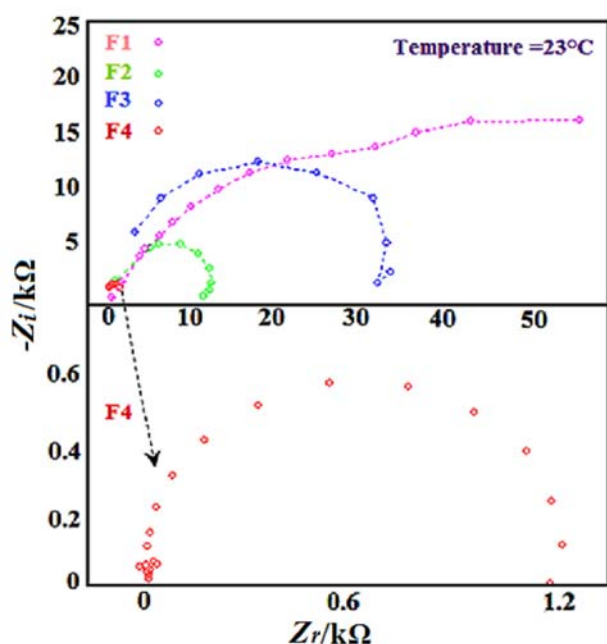
Table 1 summarises the compositions of the polymer films. Fig. 11 and Table 4 show the ionic conductivity values of the UV-cured polymer blend films with various Li-salts and 6F diacrylate prepared in

**Table 3.** Gel content and water absorption properties of UV-cured films

Formulation	Gel content/%	Water absorption/%	Total 6F diacrylate in total formulation/mass %
F1	70	8.5	–
F2	83	7.1	5
F3	87	2.4	20
F4	77	4.1	15

**Table 4.** Composition of UV-cured polymeric membranes investigated

Membrane	Polymer resin	Ethoxylated 6F diacrylate	Li-salt solution	$\sigma$ at 23°C
	g			S cm <sup>-1</sup>
F1	1	–	1	$1.41 \times 10^{-6}$
F2	1	0.1	1	$1.24 \times 10^{-5}$
F3	1	0.5	1	$4.45 \times 10^{-6}$
F4	1	0.5	2	$1.00 \times 10^{-4}$

**Fig. 11.** Typical impedance response of four polymer membranes developed in this study. Frequency: from 40 Hz to 100 mHz (see Table 1. for polymer membranes composition).

the presence of a solvent mixture of EC : DMC : PC (2 : 1 : 1 vol.) containing 1 M LiBF<sub>4</sub>–LiCF<sub>3</sub>SO<sub>3</sub> (3 : 1 molar ratio). Fig. 11 shows that membrane F4 exhibited an ionic conductivity of  $1.00 \times 10^{-4}$  S cm<sup>-1</sup> at ambient temperature, which is approximately comparable with that of common liquid electrolytes used in lithium secondary battery applications (Onishi et al., 1996; Siska & Shriver, 2001; Kang et al., 2003). Hence, UV-curing is confirmed as a suitable method for preparing membranes for use as polymer electrolytes for lithium secondary batteries. As can be

seen in Table 1, F1 and F2 formulations have different amounts of 6F diacrylate. The effect of ethylene oxide (EO) on the ionic conductivity is clearly shown in these samples. Membranes F1 and F2 exhibited ionic conductivities of  $1.41 \times 10^{-6}$  S cm<sup>-1</sup> and  $1.24 \times 10^{-5}$  S cm<sup>-1</sup>, respectively. For the F3 and F4 formulations, the ionic conductivity of the polymer solid electrolytes increases with the polarity of the matrix. For the latter, the ethoxy groups acted only as a plasticiser, which increases polymer chain flexibility and free volume. In addition, it has been reported (MacCallum et al., 1986) that conductivity initially increases with salt concentration as the number of charge carriers increases, as can be seen in the formulations of membranes F3 and F4. Hence, membranes F3 and F4 exhibited ionic conductivities of  $4.45 \times 10^{-6}$  S cm<sup>-1</sup> and  $1.00 \times 10^{-4}$  S cm<sup>-1</sup>, respectively. However, at higher salt concentrations, conductivity decreases because of the increasing influence of the ion pairs and higher ion aggregations, which reduces overall mobility and the number of effective charge carriers. This result clearly prove that the behavior of polymer electrolyte highly depends on salt concentration (Cowie & Spence, 1998; Shibata et al., 2000). Therefore, the salt concentration was maintained at appropriate value within polymer matrix in order to increase ionic conductivity as shown in Table 4.

#### *Electrochemical stability window-cyclic voltammetry (CV)*

Fig. 12 illustrates the relatively good electrochemical stability of membrane F4, as determined by CV of a SS working electrode vs a lithium foil counter electrode. The working voltage range (i.e. the electrochemical potential window) was found to be from 2.5 V to 6 V, which appears to be substantially higher than typical device application require-

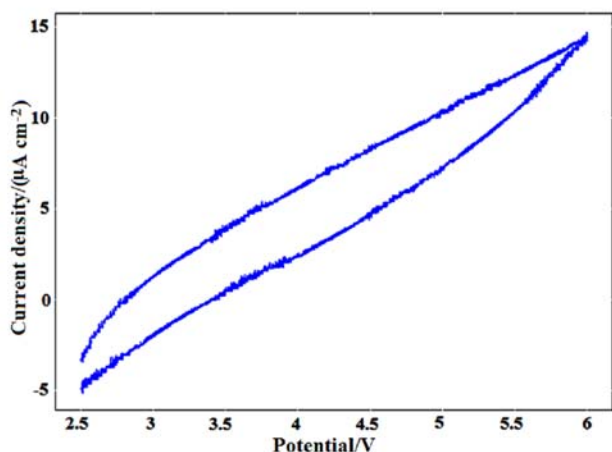


Fig. 12. Cyclic voltammogram of SS/F4/Li system at  $10 \text{ mV s}^{-1}$ .

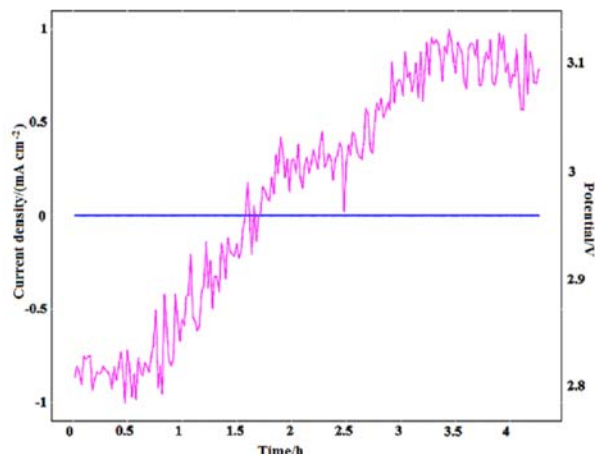


Fig. 14. Galvanostatic recurrent differential pulse of Li/PE(F4)/LiCoO<sub>2</sub> cell.

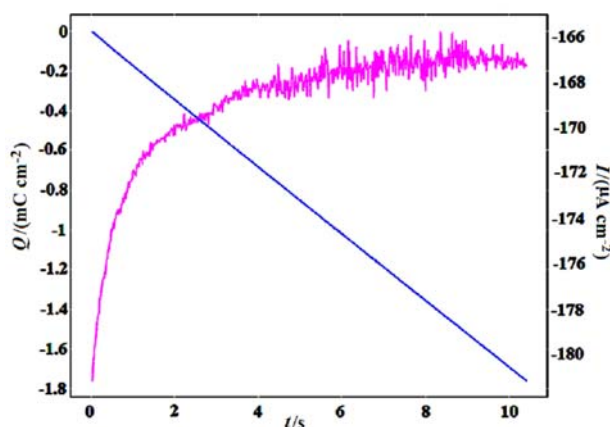


Fig. 13. Chronocoulougram and chronoamperogram of Li/PE(F4)/LiCoO<sub>2</sub> cell.

ments, particularly electrolytes in lithium rechargeable battery systems. Small currents measured extreme potentials, e.g. approximately  $15 \mu\text{A cm}^{-2}$ , at 6.0 V. On the other hand, a slight increase in current at approximately 2.8 V is assumed to be associated with the breakdown of the lithium salt and there was no evidence of significant electrochemical activity in the polymer at potentials as high as 6.0 V.

### Electrochemical analysis

As can be seen in Fig. 13, one of the important parameters for the characterisation of any polymer electrolyte is the measurement of the charge vs time response to an applied potential step waveform. The shape of the resulting chronocoulougram and chronoamperogram can be understood by considering the concentration gradients in the polymer electrolyte adjacent to the electrode surface. This was evaluated with a cell featuring a Li metal foil anode

Table 5. Performance characteristics of Li/PE(F4)/LiCoO<sub>2</sub>

Anode material	Li foil
Polymer electrolyte	F4
Cathode material	LiCoO <sub>2</sub>
Specific capacity/(mA h)	42
Specific power/(mW h)	130.2
Specific energy/J	468.72
Potential/(mV)	3100

and a LiCoO<sub>2</sub> cathode electrode by chronocoulometry and chronoamperometry.

Fig. 14 shows that the initial open circuit potential was 2.75 V and the charging process was limited to a 3.1 V cut-off potential. This was evaluated with a cell featuring a Li metal foil anode and a LiCoO<sub>2</sub> cathode electrode. Unfortunately, the potential value was insufficient; the potential required for rechargeable batteries is 3.6 V. Both the Li ions concentration polarisation in the electrolyte present in the separator and electrode and the Li ion diffusion rates in the electrode materials become important. It is clear that meeting the demand for micro- or nano-sized particles depends on the Li ions diffusion in the solid electrode particles and the desired discharge power of the battery system.

The performance characteristics of the Li/PE(F4)/LiCoO<sub>2</sub> cell are shown in Table 5. The electrochemical analysis results show that the concentration polarisation and the diffusion rates dominate the performance of the cell.

### Conclusions

UV-cured CL-based PUA polymer blend electrolytes were prepared and characterised. Free-standing flexible electrolyte films were prepared by UV-curing via free-radical photopolymerisation. Elec-

trolyte stability was demonstrated by the negligibly small currents at extreme potentials, e.g. approximately  $15 \mu\text{A cm}^{-2}$  at 6.0 V vs Li/Li<sup>+</sup>. No peaks were observed between 3.0 V and 5.0 V. The liquid electrolytes commonly used in ambient temperature rechargeable lithium-ion batteries have ionic conductivities from  $10^{-3} \text{ S cm}^{-1}$  to  $10^{-2} \text{ S cm}^{-1}$ . Therefore, to achieve the performance level of liquid electrolyte-based systems, polymer electrolytes must possess ionic conductivities that approach to or exceed  $10^{-3}$ – $10^{-4} \text{ S cm}^{-1}$  at ambient temperature. Ionic conductivities from  $10^{-6} \text{ S cm}^{-1}$  to  $10^{-4} \text{ S cm}^{-1}$  at 23°C were obtained for the membranes hence these results are comparable with those from other single-ion lithium conductive polymers (Onishi et al., 1996; Dérand et al., 1998; Siska & Shriver, 2001). Impedance measurements showed that the ionic conductivity of the polymer electrolyte was not affected by UV-curing. In addition, this process causes a decrease in the degree of crystalline structure in the polymer electrolyte, which contributes to an increase in ionic conductivity (Kang et al., 2003).

The UV-curing process affords several advantages over conventional processes used in the coating industry. These benefits include rapid application, safety, reliability and high energy efficiency because the polymerisation is performed at ambient temperature. In conclusion, the electrolyte with optimal amounts of fluorine-containing oligomer and an optimal salt mixture content exhibited an enhancement in conductivity, exhibiting a conductivity of  $1 \times 10^{-4} \text{ S cm}^{-1}$  at 23°C.

*Acknowledgements.* The financial support received from the Scientific and Technological Research Council of Turkey (research project no. 209T121) is gratefully acknowledged.

## References

- Ali, M. A., Ooi, T. L., Salmiah, A., Ishiaku, U. S., & Ishak, Z. A. M. (2001). New polyester acrylate resins from palm oil for wood coating application. *Journal of Applied Polymer Science*, 79, 2156–2163. DOI: 10.1002/1097-4628(20010321)79:12<2156::aid-app1023>3.0.co;2-k.
- Armarego, W. L. F., & Perin, D. D. (2002). *Purification of laboratory chemicals*, 4th ed. Oxford, UK: Heinemann.
- Athawale, V. D., & Raut, S. S. (2002). New interpenetrating polymer networks based on uralkyd/poly(glycidyl methacrylate). *European Polymer Journal*, 38, 2033–2040. DOI: 10.1016/s0014-3057(02)00098-8.
- Besenhard, J. O., & Winter, M. (2002). Advances in battery technology: Rechargeable magnesium batteries and novel negative-electrode materials for lithium ion batteries. *ChemPhysChem*, 3, 155–159. DOI: 10.1002/1439-7641(20020215)3:2<155::aid-cphc155>3.0.co;2-s.
- Cowie, J. M. G., & Spence, G. H. (1998). Ion conduction in macroporous polyethylene film doped with electrolytes. *Solid State Ionics*, 109, 139–144. DOI: 10.1016/s0167-2738(98)00004-6.
- de Zea Bermudez, V., Alcácer, L., Acosta, J. L., & Morales, E. (1999). Synthesis and characterization of novel urethane cross-linked ormolytes for solid-state lithium batteries. *Solid State Ionics*, 116, 197–209. DOI: 10.1016/s0167-2738(98)00346-4.
- Dérand, H., Wesslén, B., & Mellander, B. E. (1998). Ionic conductivity and dielectric properties of poly(ethylene oxide) graft copolymers end-capped with sulfonic acid. *Electrochimica Acta*, 43, 1525–1531. DOI: 10.1016/s0013-4686(97)10095-0.
- Flåtten, A., Bryhni, E. A., Kohler, A., Bjørg, E., & Isaksson, T. (2005). Determination of C22:5 and C22:6 marine fatty acids in pork fat with Fourier transform mid-infrared spectroscopy. *Meat Science*, 69, 433–440. DOI: 10.1016/j.meatsci.2004.10.002.
- Garino, N., Zanarini, S., Bodoardo, S., Nair, J. R., Pereira, S., Pereira, L., Martins, R., Fortunato, E., & Penazzi, N. (2013). Fast switching electrochromic devices containing optimized BEMA/PEGMA gel polymer electrolytes. *International Journal of Electrochemistry*, 2013, 1–10. DOI: 10.1155/2013/138753.
- Gerbaldi, C., Nair, J. R., Meligrana, G., Bongiovanni, R., Bodoardo, S., & Penazzi, N. (2009). Highly ionic conducting methacrylic-based gel-polymer electrolytes by UV-curing technique. *Journal of Applied Electrochemistry*, 39, 2199–2207. DOI: 10.1007/s10800-009-9805-6.
- Gerbaldi, C., Nair, J. R., Meligrana, G., Bongiovanni, R., Bodoardo, S., & Penazzi, N. (2010). UV-curable siloxane-acrylate gel-copolymer electrolytes for lithium-based battery applications. *Electrochimica Acta*, 55, 1460–1467. DOI: 10.1016/j.electacta.2009.05.055.
- Gite, V. V., Mahulikar, P. P., & Hundiwale, D. G. (2010). Preparation and properties of polyurethane coatings based on acrylic polyols and trimer of isophorone diisocyanate. *Progress in Organic Coatings*, 68, 307–312. DOI: 10.1016/j.porgcoat.2010.03.008.
- Gunduz, N. (1998). *Synthesis and photopolymerization of novel dimethacrylates*, Master of Science in Chemistry, dissertation. Blacksburg, VA, USA: Virginia Polytechnic Institute and State University.
- Imperiyka, M., Ahmad, A., Hanifah, S. A., & Rahman, M. Y. A. (2013). Potential of UV-curable poly(glycidyl methacrylate-co-ethyl methacrylate)-based solid polymer electrolyte for lithium ion battery application. *International Journal of Electrochemical Science*, 8, 10932–10945.
- Jia, C. K., Liu, J. G., & Yan, C. W. (2012). A multilayered membrane for vanadium redox flow battery. *Journal of Power Sources*, 203, 190–194. DOI: 10.1016/j.jpowsour.2011.10.102.
- Johnson, L. G., Allie, L. A., & Muller, J. R. (2013). U.S. Patent No. 20130011745. Washington, D.C.: U.S. Patent and Trademark Office.
- Kang, Y. K., Cheong, K. J., Noh, K. A., Lee, C. J., & Seung, D. Y. (2003). A study of cross-linked PEO gel polymer electrolytes using bisphenol A ethoxylate diacrylate: Ionic conductivity and mechanical properties. *Journal of Power Sources*, 119–121, 432–437. DOI: 10.1016/s0378-7753(03)00183-6.
- Kawaguchi, M., Fukushima, T., Miyazaki, K., Horibe, T., Habe, T., Sawamura, N., & Nagaoka, K. (1983). Synthesis and physical properties of polyfunctional methacrylates: Part II. Physical properties of 2,2-bis(4-methacryloxy cyclohexyl)propane and methyl methacrylate copolymers. *Journal of the Japanese Society for Dental Materials and Devices*, 2, 298–301.
- Kayaman-Apohan, N., Demirci, R., Çakır, M., & Gungor, A. (2005). UV-curable interpenetrating polymer networks based on acrylate/vinylether functionalized urethane oligomers. *Radiation Physics and Chemistry*, 73, 254–262. DOI: 10.1016/j.radphyschem.2004.09.026.
- Kil, E. H., Choi, K. H., Ha, H. J., Xu, S., Rogers, J. A., Kim, M. R., Lee, Y. G., Kim, K. M., Cho, K. Y., & Lee, S. Y. (2013).

- Imprintable, bendable and shape-conformable polymer electrolytes for versatile-shaped lithium-ion batteries. *Advanced Materials*, 25, 1395–1400. DOI: 10.1002/adma.201204182.
- Lin, S. B., Tsay, S. Y., Speckhard, T. A., Hwang, K. K. S., Jezerc, J. J., & Cooper, S. L. (1984). Properties of UV-cured polyurethane acrylates: Effect of polyol type and molecular weight. *Chemical Engineering Communications*, 30, 251–273. DOI: 10.1080/00986448408911131.
- MacCallum, J. R., Tomlin, A. S., & Vincent, C. A. (1986). An investigation of the conducting species in polymer electrolytes. *European Polymer Journal*, 22, 787–791. DOI: 10.1016/0014-3057(86)90017-0.
- Morales, E., & Acosta, J. L. (1999). Synthesis and characterisation of poly(methylalkoxysiloxane) solid polymer electrolytes incorporating different lithium salts. *Electrochimica Acta*, 45, 1049–1056. DOI: 10.1016/S0013-4686(99)00300-X.
- Oh, B., Jung, W. I., Kim, D. W., & Rhee, H. W. (2002). Preparation of UV curable gel polymer electrolytes and their electrochemical properties. *Bulletin of the Korean Chemical Society*, 23, 683–687.
- Onishi, K., Matsumoto, M., Nakacho, Y., & Shigehara, K. (1996). Synthesis of aluminate polymer complexes as single-ion solid electrolytes. *Chemistry of Materials*, 8, 469–472. DOI: 10.1021/cm950388a.
- Panchal, P. C., & Patel, H. S. (2013). Hybrid UV-curable poly(urethane acrylate)s surface coatings using coconut oil based alkyd resin. *Der Chemica Sinica*, 4, 52–57.
- Papke, B. L., Ratner, M. A., & Shriver, D. F. (1982). Conformation and ion-transport models for the structure and ionic conductivity in complexes of polyethers with alkali metal salts. *Journal of the Electrochemical Society*, 129, 1694–1701. DOI: 10.1149/1.2124252.
- Şabani, S., Önen, A. H., & Güngör, A. (2012). Preparation of hyperbranched polyester polyol-based urethane acrylates and applications on UV-curable wood coatings. *Journal of Coatings Technology and Research*, 9, 703–716. DOI: 10.1007/s11998-012-9418-6.
- Santhosh, P., Vasudevan, T., Gopalan, A., & Lee, K. P. (2006). Preparation and properties of new cross-linked polyurethane acrylate electrolytes for lithium batteries. *Journal of Power Sources*, 160, 609–620. DOI: 10.1016/j.jpowsour.2006.01.091.
- Scrosati, B. (1993). *Applications of electroactive polymers*. London, UK: Chapman and Hall.
- Scrosati, B. (1995). Challenge of portable power. *Nature*, 373, 557–558. DOI: 10.1038/373557a0.
- Seo, J. C., Jang, E. S., Song, J. H., Choi, S. H., Khan, S. B., & Han, H. S. (2010). Preparation and properties of poly(urethane acrylate) films for ultraviolet-curable coatings. *Journal of Applied Polymer Science*, 118, 2454–2460. DOI: 10.1002/app.32344.
- Shibata, M., Kobayashi, T., Yosomiya, R., & Seki, M. (2000). Polymer electrolytes based on blends of poly(ether urethane) and polysiloxanes. *European Polymer Journal*, 36, 485–490. DOI: 10.1016/S0014-3057(99)00101-9.
- Silva, M. M., Barros, S. C., Smith, M. J., & MacCallum, J. R. (2002). Study of novel lithium salt-based, plasticized polymer electrolytes. *Journal of Power Sources*, 111, 52–57. DOI: 10.1016/S0378-7753(02)00229-X.
- Siska, D. P., & Shriver, D. F., & (2001). Li<sup>+</sup> conductivity of polysiloxane-trifluoromethylsulfonamide polyelectrolytes. *Chemistry of Materials*, 13, 4698–4700. DOI: 10.1021/cm000420n.
- Sultan, M., Zia, K. M., Bhatti, H. N., Jamil, T., Hussain, R., & Zuber, M. (2012). Modification of cellulosic fiber with polyurethane acrylate copolymers. Part I: Physicochemical properties. *Carbohydrate Polymers*, 87, 397–404. DOI: 10.1016/j.carbpol.2011.07.070.
- Tabasum, S., Zuber, M., Jabbar, A., & Zia, K. M. (2013). Properties of the modified cellulosic fabrics using polyurethane acrylate copolymers. *Carbohydrate Polymers*, 94, 866–873. DOI: 10.1016/j.carbpol.2013.01.087.
- Uğur, M. H., Toker, R. D., Kayaman-Apohan, N., & Güngör, A. (2014). Preparation and characterization of novel thermoset polyimide and polyimide-peo doped with LiCF<sub>3</sub>SO<sub>3</sub>. *eXPRESS Polymer Letters*, 8, 123–132. DOI: 10.3144/expresspolymlett.2014.15.
- Xu, W., Belieres, J. P., & Angell, C. A. (2001). Ionic conductivity and electrochemical stability of poly[oligo(ethylene glycol)oxalate]-lithium salt complexes. *Chemistry of Materials*, 13, 575–580. DOI: 10.1021/cm000694a.
- Yang, Z. G., Zhang, J. L., Kinter-Meyer, M. C. W., Lu, X. C., Choi, D. W., Lemmon, J. P., & Liu, J. (2011). Electrochemical energy storage for green grid. *Chemical Reviews*, 111, 3577–3613. DOI: 10.1021/cr100290v.
- Yildiz, E., Güngör, A., Yildirim, H., & Baysal, B. M. (1995). Synthesis and characterization of UV curable acrylated urethane prepolymers, II. Effects of various diacrylates as diluents and relative humidity on mechanical properties of TDI/PEG/HEMA-based polymeric films. *Die Angewandte Makromolekulare Chemie*, 233, 33–45. DOI: 10.1002/apmc.1995.052330104.
- Zhang, S. S., Xu, K., & Jow, T. R. (2002). A new approach toward improved low temperature performance of Li-ion battery. *Electrochemistry Communications*, 4, 928–932. DOI: 10.1016/S1388-2481(02)00490-3.